International Journal of Recent Technology and Engineering (IJRTE)
ISSN: 2277-3878 (Online), Volume-8 Issue-4, November 2019

Dynamic Monitoring of the Effect of Passenger Occupancy on the Vehicle Center of Gravity (CG) In a Lightweight Electric Vehicle

Sujan Neroula, Chinmayee Hazarika, Santanu Sharma

Abstract: *In lightweight vehicles, the passenger weight has a substantial contribution to the vehicle gross weight. This paper presents a simulation, evaluation, and application of vehicle model developed to estimate the shift in the center of gravity (CG) of the vehicle on various terrains, driving conditions and different passenger occupancy combinations. The designed Neighbourhood Electric Vehicle (NEV) comprises various sensors including load sensors and speed sensors at each wheel. Vehicle dynamics is influenced by various factor like speed, goad grade, lateral acceleration, longitudinal acceleration, passenger occupancy, etc. Here a simple model has been presented where the movement of the vehicle CG is mapped based on the load experienced by each wheel in dynamic driving conditions. The wheel forces are used to identify the instantaneous CG by virtue of a system identifier on board the vehicle. The validation of the proposed model has been done on a lightweight NEV. In addition, several simulations have been carried out to illustrate the effect on vehicle dynamic stability. It was found that the passenger occupancy status can influence vehicle performance and handling to a large extent.*

Keywords **:** *Passenger occupancy, vehicle dynamics, wheel load sensor, centre of gravity, traction control, electronic brake force distribution (EBD).*

I. INTRODUCTION

Studies claim that in order to prevent catastrophic climate change, the current level of greenhouse gas (GHG) emissions must be cut down by 60% by the year 2050 [1]. Vehicles are amongst the foremost sources of air pollution as the transport sector alone causes 33.7% of GHG emission and contribute approximately 27% to the world energy consumption [2]. With the growing concern for environment and decline in petroleum reserves, more efficient and lightweight vehicles are getting an overwhelming response. Electrifying the vehicle driveline is one of the promising approaches with many benefits, as the use of more efficient drivetrain and electric motor show better performance than the internal combustion engine vehicles (ICEVs) [3]. The key difference between an electric vehicle (EV) and ICEV is that the EVs are fully or partially driven by an electric motor that can cater the ability to dynamic traction control. Other unique advantages of using an electric motor in vehicle drivetrain are; faster torque response, ease of implementation and ability of a motor to produce traction as well as braking force (regenerative braking) [4]. Use of strong and lightweight materials in vehicle manufacturing has significantly downsized the vehicle weight with a positive impact on the overall efficiency.

In recent times, many works reported in the national and international arena are on the autonomous driving vehicles. A self-driving vehicle has the capability to perceive the surrounding environment and navigate without any human interventions [5]. There must be a relation between the steering angle and driver's view [6], may it be a human or any image processing technique used for the autonomous driving vehicle. Sensors like the optical rangefinder and odometry sensors can be used to make collision-free manoeuvre consisting of arc and segments [7]. The development of obstacle and pedestrian detection can be significantly advanced using the deep learning approaches, such as; Single Shot Detector (SSD), Fast Region-Convolutional Neural Network (R-CNN) and Faster R-CNN [8]. In addition to these, the tyre road frictional coefficient plays an important role in realizing the idea of automated vehicle [9]. However, in all the above reported work on the autonomous vehicles, the variation in the vehicle CG due to passenger occupancy has not been taken into account.

Reduction in the vehicle weight has a positive impact on the overall efficiency, on the other hand, reduced kerb weight increases the significance of the weight of passengers onboard. In this paper, the effect on vehicle efficiency and dynamics caused by the shift in CG of a vehicle due to variation in passenger occupancy and passenger weight has been presented. Studies claim that vehicles such as sports utility vehicles (SUV), vans and mini trucks are more prone to rollover incidents due to their higher CG [10]. The rollover incidents occurred only in 2.3% of the total incidents involving these vehicles whereas the fatality rate was about 10.6% [10, 11]. Also, it was observed in our work that the CG position in the lightweight vehicle significantly varies with different occupancy configurations.

Manuscript published on November 30, 2019.
***** Correspondence Author

Sujan Neroula, Department of Electronics and Communication Engineering, Tezpur University, Tezpur, India.

Chinmayee Hazarika, Department of Electronics and Communication Engineering, G.I.M.T, Guwahati , Assam, India

Santanu Sharma*, Department of Electronics and Communication Engineering, Tezpur University, Tezpur, India.

The deviation from the mean position in the worst-case scenario was about 18.6 cm, for a vehicle parked on the leveled road. This deviation goes even further when the vehicle is subjected to higher acceleration, inclined terrains, and sharp turns.

In this framework, the following sections of the paper comprise of vehicle wheel load estimation, suspension modeling followed by results and discussion.

II. NEV DESIGN PARAMETERS

A. NEV design

A lightweight electric vehicle has been designed with independently driven rear wheels with a fixed transmission ratio of 10:1. The vehicle is designed with five seats and seats have been indexed as S_1-S_5. The vehicle parameters are illustrated in Table I.

Table-I: Vehicle parameters, values and units

Parameters		Values	Unit
Vehicle mass	*M*	300	kg
Passenger mass	*m*	70	kg
Wheel base	*L*	1.7	m
Track width	*T*	0.92	m
position of each wheel	*FL*	0.966 $\angle 61.57^0$	m
	FR	0.966 $\angle 118.42^0$	m
	RL	0.966 $\angle -118.42^0$	m
	RR	0.966 $\angle -61.57^0$	m
position of each seat	S_1	0.67 $\angle 63.43^0$	m
	S_2	0.67 $\angle 116.56^0$	m
	S_3	0.67 $\angle -116.56^0$	m
	S_4	0.6 $\angle -90$	m
	S_5	0.67 $\angle -63.43^0$	m

The vehicle is designed such that the CG of the unoccupied vehicle lies on the roll axis of the vehicle, the placements of various vehicle components like the vehicle Electronic Control Unit (ECU) and batteries are made such that the CG lies equidistant from all vehicle wheels. The seating positions are designed such that it doesn't bring about any change in the designed CG position in the unloaded vehicle. The vehicle wheels are equipped with load cells and speed sensors, the load cell and speed sensor transmit the data to the ECU of the vehicle which is further processed to design a driving strategy for the vehicle.

B. NEV drive circuit

This section illustrates the first quadrant chopper drive designed to drive the vehicle. The motor driver section is optically isolated from the high power section using optical-isolators. The vehicle can experience many situations where the motor current can exceed the limit of a single MOSFET, to handle such scenarios, six IRF3205 power MOSFET has been used in parallel. This enhances the current handling capacity of the drive and also cuts down the channel resistance. Use of multiple MOSFET requires a higher gate current in high-frequency operations. A gate drive circuit has been designed to meet this high demand of gate current. The complete circuit has been illustrated in figure 1.

Switching with an inductive load like PMDC motor at higher frequencies brings about many challenges like peak overshoot and ringing. With the intention to enhance the efficiency and to ensure the safe operation of the drives, voltage overshoot and ringing must be minimized. A Resistor Capacitor Diode (RCD) turn off (voltage), snubber has been used to minimize the system ringing and suppress the peak voltage overshoot.

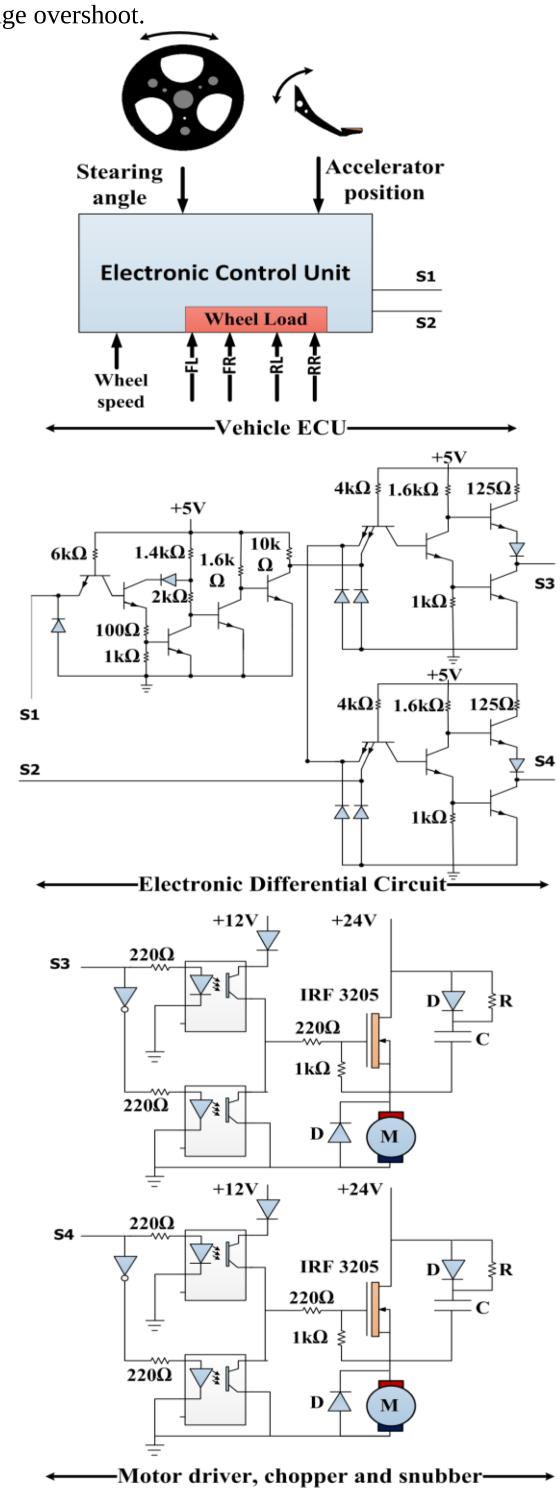

Fig. 1.

The complete schematics of the circuit used to drive the vehicle comprising the input section to implement differential action and ECU, the gate driver circuit, the low side PWM chopper drive, and the RCD snubber circuit

III. VEHICLE SUSPENSION MODELING

Lagrange's model has been used to model the suspension of the designed vehicle. This model proves to be an effective approach when the suspension is modeled neglecting the mass of the wheel and roll moment. This model also takes into account the damping and stiffness of the suspension along with the vehicle pitch.

The values for the spring constant and damping coefficient of the suspension systems are K_S=3900 Nm^{-1} and b_r, b_f=2000 N-sm^{-1} respectively. The model has been illustrated in figure 2(a).

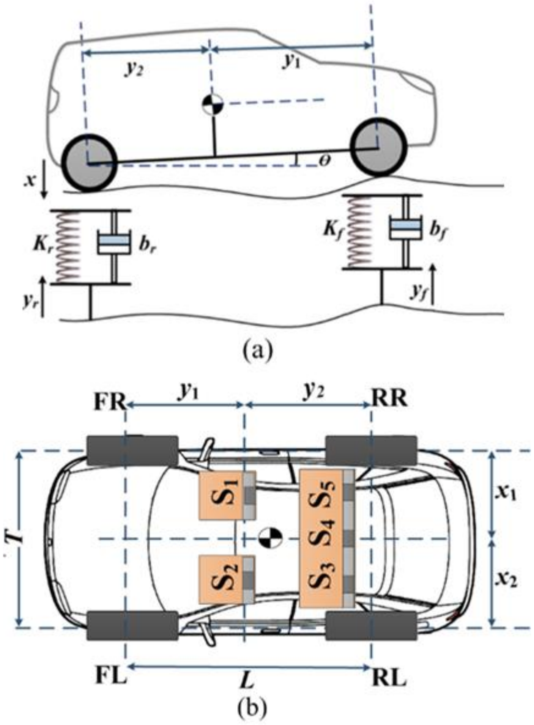

Fig. 2. (a) Suspension modelling by Lagrange's model. (b) Passenger seating positions and vehicle parameters.

The indexing *f* and *r* refer the front and rear of the vehicle respectively. The moment of inertia, *I* for the designed vehicle has been measured to be 144.5 kg.m^2. Equation 1 is the final derived equation for the suspension model.

$$\begin{bmatrix} M & 0 \\ 0 & I \end{bmatrix} = \begin{bmatrix} \ddot{x} \\ \ddot{\theta} \end{bmatrix} + \begin{bmatrix} b_f + b_r & y_2 b_r - y_1 b_f \\ y_2 b_r - y_1 b_f & y_2{}^2 b_r + y_1{}^2 b_f \end{bmatrix} \begin{bmatrix} \dot{x} \\ \dot{\theta} \end{bmatrix}$$
$$+ \begin{bmatrix} K_f + K_r & K_r y_2 - K_f y_1 \\ K_r y_2 - K_f y_1 & y_1{}^2 K_f + y_2{}^2 K_r \end{bmatrix} \begin{bmatrix} x \\ \theta \end{bmatrix}$$
$$= \begin{bmatrix} K_f & K_r \\ -K_f y_1 & K_r y_2 \end{bmatrix} \begin{bmatrix} y_f \\ y_r \end{bmatrix} + \begin{bmatrix} b_f & b_r \\ -b_f y_1 & b_r y_2 \end{bmatrix} \begin{bmatrix} \dot{y}_f \\ \dot{y}_r \end{bmatrix}$$

(1)

The damping coefficient and natural frequency for equation 1 has been found to be

$$\zeta_1 = 0.75,\ \ \zeta_2 = 0.22$$

$$\omega_{n1} = 11.15\, rad\ s^{-1},\ \ \omega_{n2} = 16.88\, rad\ s^{-1}$$

Two transfer function exists for the two damping coefficients and natural frequencies i.e.

$$H_1(s) = \frac{284.9}{s^2 + 7.43s + 284.9},$$

$$H_2(s) = \frac{124.2}{s^2 + 16.7s + 124.2} \qquad (2)$$

A unit signal can be used to illustrate the performance of the suspension model. This has been achieved by designing an obstacle that resembles a unit input signal. The vehicle is driven over an obstacle of height 2.4cm, at speed of 5ms^{-1} and the response of the load cells associated with each wheel, has been recorded in real-time. It was observed that the recorded response closely resembles the expected damping coefficient and natural frequencies of the suspension model as illustrated in figure 3.

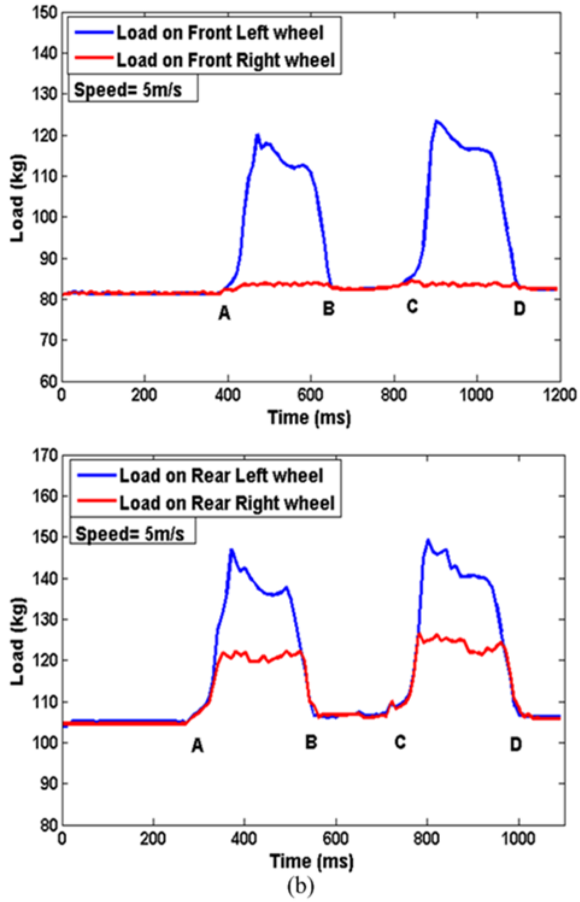

Fig. 3. (a) Sensor response when front wheel passes over two consecutive obstacles of height 2.4cm and 500cm wide at speed of 5ms^{-1}. (b) Sensor response when rear wheels passing over two consecutive obstacles of height 2.4cm and 500cm wide at speed of 5ms^{-1}.

The normal load on the front and rear wheels also vary whenever the vehicle accelerates or decelerates, in addition to the pitch caused by the torque developed about the axis of the rear axle, the height of the CG also has a major role in this. For this reason, the vehicle is designed with a lower CG of 0.32m.

IV. DETERMINATION OF VEHICLE CG

The load on a wheel of a vehicle parked on the levelled road is the function of the position of vehicle CG and hence, the coordinates of the later can be expressed as the function of the former. Equation 4 represents the load on each wheel as a function of the coordinates of vehicle CG [12].

$$\begin{bmatrix} F_{FL} \\ F_{FR} \\ F_{RL} \\ F_{RR} \end{bmatrix} = \frac{m\,g}{LT} \begin{bmatrix} y_2 x_1 \\ y_2 x_2 \\ y_1 x_1 \\ y_1 x_2 \end{bmatrix} \quad (4)$$

Here the LHS of the equation describes the force on each wheel as the function of the coordinates of the CG. This equation has been used to design the system identifier that estimates the vehicle coordinates of the CG using the data from the wheel load sensors.

Figure 4 illustrates the different driving situations and the movement of vehicle CG in these conditions.

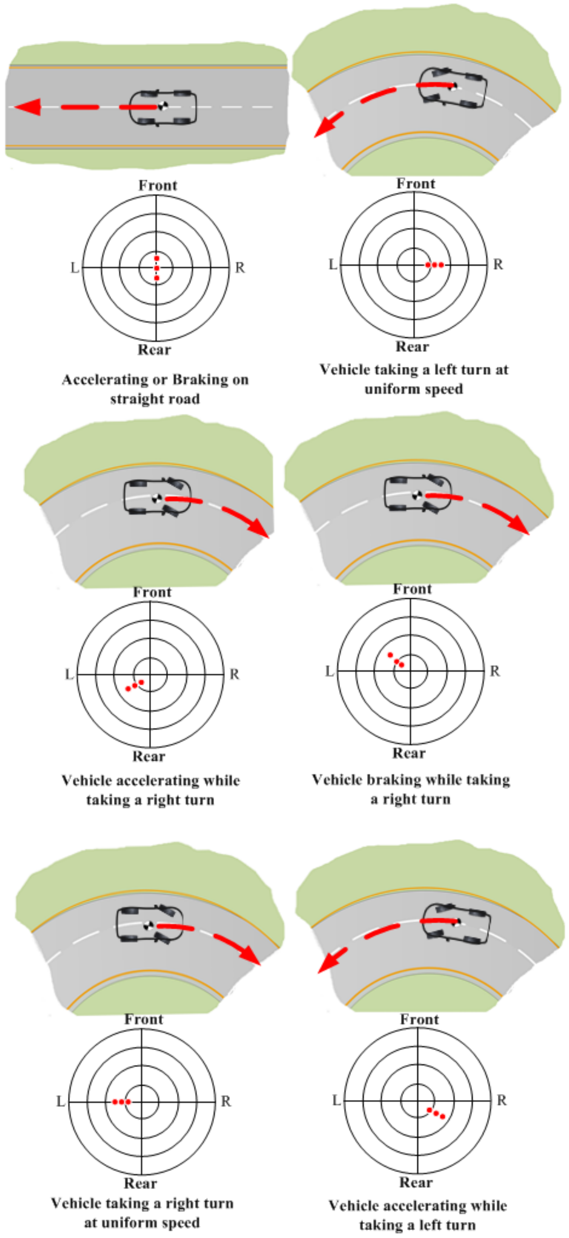

Fig. 4. Apparent shift in the position of CG during different manoeuvres.

V. RESULTS AND DISCUSSION

A. Determination of vehicle CG under different occupancy conditions.

Considering the driver's seat (S_1) to be always occupied, the remaining seats (S_2, S_3, S_4, and S_5) can be occupied or can be vacant as per the requirements. These remaining four seats can be occupied in 16 different combinations. Table II illustrates the seating configurations for all 16 combinations. Here the occupancy has been expressed in binary where; 1: the occupied seat, 0: vacant seat.

For all the 16 possible passenger occupancy combinations, the vehicle can have 16 different positions of CG. If the vehicle CG without any occupant is considered to be at the origin, the simulation results in CG positions for these 16 combinations are depicted in figure 5(a).

A test has been carried out on a stationary vehicle with different passenger occupancies. Figure 5(b) compares the simulation results and the actual results for the CG positions. However, the CG position changes when the vehicle undergoes a left or right turn at higher speed, leading to a significant change in wheel load. While negotiating a left turn, the outer wheel (right wheel) experiences higher load and on the other hand, the load on the inner wheels (left wheel) decreases. These wheel loads can be used to determine the instantaneous vehicle CG (when compared to the vehicle parked on the levelled surface). The MATLAB system identifier is used to determine the vehicle CG, with load from the four wheels as inputs. Figure 6(a) illustrates the position of vehicle CG during a left turn at speed of $15ms^{-1}$ with a turning radius of 100m

Table- II: Different seating configuration of the five seats, 1: occupied, 0: vacant.

S. No	Occupancy status				
	S_5	S_4	S_3	S_2	S_1
1	0	0	0	0	1
2	0	0	0	1	1
3	0	0	1	0	1
4	0	0	1	1	1
5	0	1	0	0	1
6	0	1	0	1	1
7	0	1	1	0	1
8	0	1	1	1	1
9	1	0	0	0	1
10	1	0	0	1	1
11	1	0	1	0	1
12	1	0	1	1	1
13	1	1	0	0	1
14	1	1	0	1	1
15	1	1	1	0	1
16	1	1	1	1	1

When the vehicle undergoes a right turn of radius 100m with a speed of $15ms^{-1}$, the outer wheels (left wheel) experiences higher load and the load on inner wheels (right wheel) decreases. The vehicle CG in this condition is as illustrated in figure 5(b). These results are obtained from the simulation in MATLAB with a vehicle parameter considered the same as that of the designed vehicle.

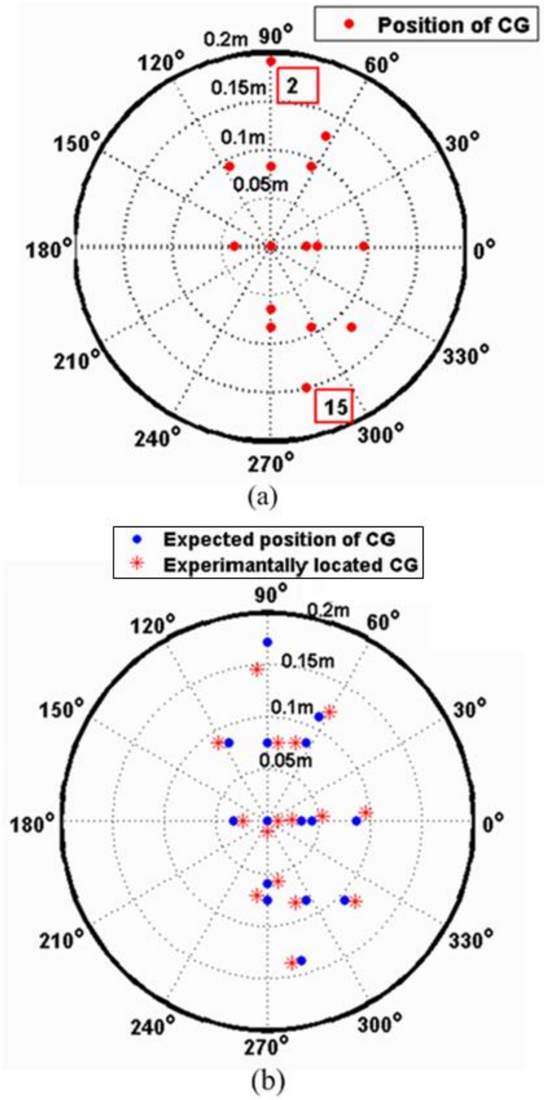

Fig. 5. (a)

Mathematical simulation to determine the vehicle CG positions for all 16 possible combinations. (b) Experimentally determined CG positions along with the mathematical simulation to determine the vehicle CG positions for all 16 possible combinations.

B. Dynamic estimation of vehicle CG under different occupancy conditions.

Two different experimental verification of the proposed idea has been carried out; firstly, the vehicle CG is plotted for all 16 occupancy combinations using the data obtained from the load sensors. Followed by experimental on-road verification of CG shift, when the vehicle is undergoing a left and right turning manoeuvre.

Dummy weight has been used as occupants to carry out few occupancy combinations. As the maximum deviation from the mean position was observed for combination 2 (only seat S_1 and S_2 occupied) and combination 15 (only S_2 vacant), the on-road tests for left and right turning manoeuvre were carried out for these two cases. The track chosen for the on-road test has a radius of 97.6± 2.7m, which is close to 100m radius considered for the simulation. No considerable road grade, undulations, and banking were present in the road considered to carry out the tests.

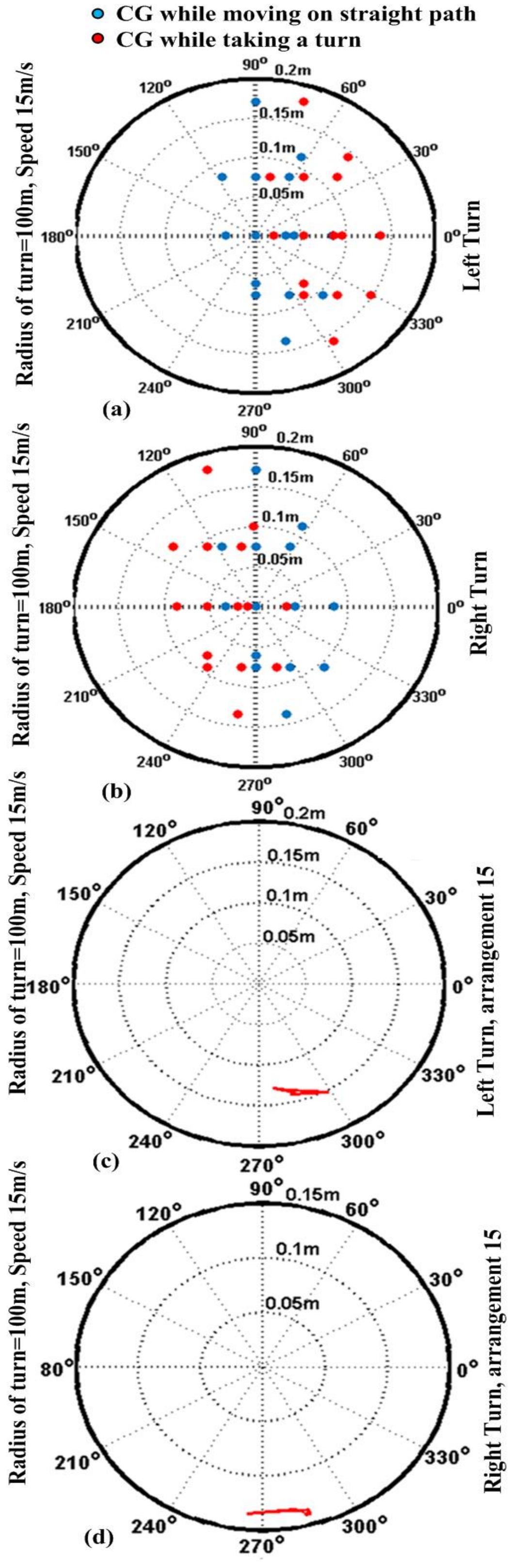

Fig. 6. (a)

Mathematical simulation to determine the vehicle CG positions for all 16 possible combinations during a left turn at speed of $15ms^{-1}$ on a turning radius of 100m. (b) Mathematical simulation to determine the vehicle CG positions for all 16 possible combinations during a left turn at speed of $15ms^{-1}$ on a turning radius of 100m. (c) Practically estimated positions of CG for a vehicle undergoing left turn at speed of $15ms^{-1}$ with seat S_1,

S_3, S_4, and S_5 occupied (d) practically estimated positions of CG for a vehicle undergoing right turn at speed of $15ms^{-1}$ with seat S_1, S_3, S_4, and S_5 occupied.

The path traced by the CG during the left turn and right turn has been illustrated in figure. 4(c) and 4(d) respectively. The tracking of CG in real-time for all passenger occupancy conditions can lead to effective implementation of traction control strategies in a lightweight electric vehicle and enhance vehicle efficiency and safety.

In addition, real-time tracking of the wheel-load can enhance vehicle braking performance as this information can enhance the performance of vehicle Anti-lock Braking System (ABS) and Electronic Brake-force Distribution (EBD).

VI. CONCLUSIONS

Vehicle traction control based on the passenger occupancy exhibits some promising results when simulations were carried out. The same model has been implemented on a developed NEV with independently driven rear wheels. The results are in considerable agreement with the simulation results. As the on-road conditions can be highly intuitive and hence comparison of the two results exhibited a small margin of error. The results of this work can be concluded as; **a)** the passenger occupancy combination can affect the vehicle CG position to a large extent in the lightweight vehicle. **b)** the seating of the passenger must be symmetrical about the vehicle roll axis to enhance the vehicle braking and traction control, and **c)** taking the seat occupancy, vehicle speed and turning radius as factors, the vehicle CG position can be traced very effectively and can be used to enhance the performance of ABS, EBD dynamic traction control and active torque vectoring.

REFERENCES

1. Bayindir, K.Ç., Gözüküçük, M.A., Teke, A.: "A comprehensive overview of hybrid electric vehicle: Powertrain configurations, powertrain control techniques and electronic control units." Energy Conversion and Management. 52, 2011, pp 1305–1313.
2. S. F. Tie and C. W. Tan, "A review of energy sources and energy management system in electric vehicles," Renewable and Sustainable Energy Reviews, vol. 20, 2013, pp. 82–102.
3. J. Y. Yong, V. K. Ramachandaramurthy, K. M. Tan, and N. Mithulananthan, "A review on the state-of-the-art technologies of electric vehicle, its impacts and prospects," Renewable and Sustainable Energy Reviews, vol. 49, 2015 pp. 365–385.
4. M. H. Sekour, K. Hartani, and A. Merah, "Electric Vehicle Longitudinal Stability Control Based on a New Multimachine Nonlinear Model Predictive Direct Torque Control," Journal of Advanced Transportation, vol. 2017, pp. 1–19.
5. K. Jo, J. Kim, D. Kim, C. Jang, and M. Sunwoo, "Development of Autonomous Car—Part I: Distributed System Architecture and Development Process," IEEE Transactions on Industrial Electronics, vol. 61, no. 12, ,2014, pp. 7131–7140.
6. K. Jo, J. Kim, D. Kim, C. Jang, and M. Sunwoo, "Development of Autonomous Car—Part I: Distributed System Architecture and Development Process," IEEE Transactions on Industrial Electronics, vol. 61, no. 12, 2014, pp. 7131–7140.
7. I. Cox, "Blanche-an experiment in guidance and navigation of an autonomous robot vehicle," IEEE Transactions on Robotics and Automation, vol. 7, no. 2, 1991, pp. 193–204.
8. S. Ahmed, M. N. Huda, S. Rajbhandari, C. Saha, M. Elshaw, and S. Kanarachos, "Pedestrian and Cyclist Detection and Intent Estimation for Autonomous Vehicles: A Survey," Applied Sciences, vol. 9, no. 11, 2019, p. 2335, Jun.
9. R. Wang and J. Wang, "Tire–road friction coefficient and tire cornering stiffness estimation based on longitudinal tire force difference generation," Control Engineering Practice, vol. 21, no. 1, 2013, pp. 65–75.
10. S. Solmaz, M. Akar, R. Shorten, and J. Kalkkuhl, "Real-time multiple-model estimation of centre of gravity position in automotive vehicles," Vehicle System Dynamics, vol. 46, no. 9, 2008, pp. 763–788.
11. D. C. Viano and C. S. Parenteau, "Rear-Seat Occupant Responses in NHTSA Rear Crash Tests," SAE Technical Paper Series, Mar. 2018.
12. R. N. Jazar, "Mathematical Theory of Autodriver for Autonomous Vehicles," Journal of Vibration and Control, vol. 16, no. 2, 2009, pp. 253–279.

AUTHORS PROFILE

Sujan Neroula received his B-Tech degree in 2012 and has done his M-tech in Electronics Design and Technology, from Tezpur University in the year 2016, currently he is doing Ph.D. in department of Electronics and Communication Engineering, Tezpur University since 2016. His area of interests include Electric vehicle, Power Electronics, vehicle dynamics, and semiconductor devices.

Chinmayee Hazarika received the B.E. degree in Electronics and Communication Engineering from K.C.G College of Technology, Tamil Nadu, India (Anna University) in 2007 and M.-Tech degree in Electronics design and technology from Tezpur University, Tezpur, India, in 2011. From 2011 to 2015 she was an Assistant Professor with the Electronics and Communication Engineering Department, Dibrugarh University, Dibrugarh, Assam, India. Her research interests include device modeling, fabrication of micro- and nano structures, biosensors, ion sensitive FETs, Enzyme FETs. Currently she is working as assistant professor with Electronics and Communication Engineering Department in Girijananda Institute of Management and Technology, Guwahati, Assam, India.

Santanu Sharma received the B.E degree in Electrical Engineering from Jorhat Engineering College, Jorhat, Assam, India (Dibrugarh University) in 1998 And M.-Tech degree in Electronics design and technology from Tezpur University, Tezpur, India, in 2000 and the Ph.D. degree in Electronics and Communication engineering from Tezpur University, in 2010.
He was a project staff in International Centre for Radio Science, Jodhpur, from July 2000 to December 2000.He was also working as Engineering Assistant at Prasar Bharati, Broadcasting Corporation of India, AIR, from December 2000 to November 2001. From December 2001 to January 2010 he was an Assistant Professor with the Electronics and Communication Engineering Department, Tezpur University, Tezpur. Currently, he is working as an Associate Professor in the same department. His area of research includes semiconductor devices, bioelectronics devices, electric vehicle and power electronics.